Desalination and Water Treatment
www.deswater.com

doi: 10.5004/dwt.2017.21433

88 (2017) 257–267
September

Adsorption behavior of perchlorate removal from aqueous solution using MgAlCe hydrotalcite-like compounds

Yiqiong Yang[a], Dewei Wen[a], Qiao Ding[a], Yin Wang[a], Ning Liu[a], Yunxiao Zhao[b,*], Xiaodong Zhang[a,*]

[a]*School of Environment and Architecture, University of Shanghai for Science and Technology, Shanghai 200093, China, email: yangyiqiong@usst.edu.cn (Y. Yang), 253751902@qq.com (D. Wen), 2389471213@qq.com (Q. Ding), 625xiaogui@163.com (Y. Wang), liuning6910@163.com (N. Liu), Tel. +86 15921267160, Fax. +86 021 55275979, email: fatzhxd@126.com (X. Zhang)*
[b]*Shanghai SINAP Membrane Tech Co., Ltd., Shanghai, 200942, China, email: yunxiao_zhao@163.com (Y. Zhao)*

Received 8 March 2017; Accepted 16 September 2017

ABSTRACT

A series of MgAlCe hydrotalcite-like compounds (HMAC) with different Mg/Al/Ce ratios were prepared via co-precipitation method, and their calcination products (CHMAC) were used as an adsorbent to remove perchlorate anionic pollutant from aqueous solution. The HMAC, CHMAC and reconstructed CHMAC were characterized by XRD, FT-IR spectra, TG and DTA. The characterization results displayed that the layered double hydroxides structures in the HMAC were lost during calcination at 600°C, but were reconstructed subsequent to adsorption of perchlorate, which was primary driven by the "reformation effect" of HMAC with perchlorate as an interlayer anion. Batch adsorption studies were performed, and the reactivity and mechanism were discussed regarding the effect of various equilibration conditions, such as adsorbent dosage, initial solution pH, initial perchlorate concentration, co-existing anions, temperature and contact time. It was found that the existence of Ce^{3+} in CHMAC was favorable to removal of perchlorate from water, and the best ratio of Mg/Al/Ce is 3:0.8:0.2 (CHMAFC). The equilibrium adsorption data fitted well to the Freundlich model and the experimental data revealed a good compliance with the pseudo-first-order kinetic model. Thermodynamic parameters ($\Delta G°$, $\Delta H°$ and $\Delta S°$) indicated that the adsorption process was endothermic and spontaneous in nature. The calcination product of MgAlCe hydrotalcite-like compound was a promising adsorbent for perchlorate anionic pollutant.

Keywords: MgAlCe hydrotalcite-like compounds; Adsorption; Calcination; Perchlorate

1. Introduction

Perchlorate has been regarded as anionic inorganic contaminant, which widely existed in drinking water, surface water, ground water, vegetation, soil, and food et al. [1,2]. Perchlorate, is frequently used as addition agent in electroplate liquid, fabric fixative, lubricants, paints, dyes, leather tanning agents and rubber product, which is widely applied in blasting operation, arms industry, firework and rocker booster [3]. Interestingly, an inorganic endocrine disruptor perchlorate can interfere with iodide uptake by the thyroid cells, consequently leading to a variety of diseases, such as, anemia and neurological damage [4]. The presence of perchlorate in the environment is detrimental to human health as it can alter hormonal balances and impede human reproduction and development [5]. Nowadays, perchlorate pollution problem has attracted worldwide attention in many countries, for example, USA [6], Germany [7], India [8], Korea [9], Japan [10], and China [11]. The removal of perchlorate is a great challenge of environmental protection because of its high mobility and stability. There is very limited regulation of perchlorate worldwide. Canada monitors perchlorate levels in drinking water and targets a recommended threshold of less than 6 mg/l, but this recommendation is not enforced [12]. Therefore, a variety of treatment

---

*Corresponding author.

1944-3994 / 1944-3986

technologies have been developed to remove perchlorate from drinking water. All technologies available for perchlorate removal or destruction in water can be classified into physical removal, chemical reduction, biodegradation, electrochemical reduction, bioelectrochemistry reduction and integrated technologies [13]. Some of these methods include adsorption using calcite [14], activated carbon [15], nano-Al_2O_3 [16], Metal organic frameworks [17], iron oxide tailings [18], zirconium hydroxide [19] and reduction using zero-valent iron or iron at high temperature [20,21], ultraviolet light [22] or biological reduction [23].

Layered double hydroxides (LDHs) can be expressed by the general formula $[M_{1-x}^{2+}M_x^{3+}(OH)_2]^{x+}[A_{x/n}^{n-}]\cdot yH_2O$, where M^{2+} and M^{3+} are divalent and trivalent metal ions in the octahedral positions of brucite-like layers yielding excessive positive charge, and A^{n-} represents the interlayer anion to balance the positive charges [24]. Due to low-cost, easy synthesis, controllability and potential recycle of layers interval, LDHs have proved to be effective and excellent adsorption materials for capturing anions [25,26]. Recently, perchlorate removal using MgAl calcined layered double hydroxides (CLDHs), MgFe CLDHs, MgAlFe CLDHs, and Zn–Al CLDHs has also been performed [27–33]. It is found that perchlorate is more effectively removed by these CLDHs than LDHs, which may be attributed to the structural reconstruction of LDHs, such as "structure reformation effect". Previous studies indicated that a drawback has limited application of the Al based ones such as MgAl hydrotalcites and their calcined products in drinking water treatment. Al could potentially develop or accelerate the Alzheimer syndrome in human beings [34]. Therefore, in order to reduce Al content of LDHs, we select rare earth Ce to partly substitute Al.

Here, a series of MgAlCe hydrotalcite-like compounds (HMAC) with different Mg/Al/Ce ratios were prepared via co-precipitation method, and their calcination products (CHMAC) were used as an adsorbent to remove perchlorate anionic pollutant from aqueous solution. The HMAC, CHMAC and reconstructed CHMAC were characterized by XRD, FT-IR spectra, TG and DTA. Batch adsorption studies were performed, and the reactivity and mechanism were discussed regarding the effect of various equilibration conditions, such as adsorbent dosage, initial solution pH, initial perchlorate concentration, co-existing anions, temperature and contact time. In addition, the isotherm patterns, kinetics and thermodynamic parameters of perchlorate adsorption on the calcined MgAlCe hydrotalcite compounds (CHMAC) were determined.

2. Experimental

2.1. Catalyst preparation

In the present study, the layered double hydroxides MgAlCe LDHs (HMACx; here, x is the mol.% of Ce) with different Mg^{2+}:Al^{3+}:Ce^{3+} molar ratios (3:0.8:0.2, 3:0.6:0.4 and 3:0.2:0.8) were prepared by low supersaturation co-precipitation method at constant pH [27]. The mixed solution containing metal nitrates of Mg^{2+}, Al^{3+} and Fe^{3+} with desired concentrations ([Mg]+[Al]+[Ce]=1 mol), 0.5 mol Na_2CO_3 and 2 mol NaOH were added simultaneously to a 1 L beaker under constant vigorous stirring condition (the rate 50 mL/h) at 75ºC, and the pH value was maintained at 7–8. The precipitate formed was aged for 24 h at 75ºC at the end of which the precipitate was separated by filter. This was followed by repeated washing with deionized water until the effluent solution was neutral. The wet solid was slowly dried at 100ºC for 24 h to obtain the HMAC. The HAMC was calcined at 600ºC for 4 h to obtain the calcined hydrotalcites signed as CHMACx (here, x is the mol. % of Ce).

2.2. Catalysts characterization

Powder X-ray diffraction (XRD) analysis was performed using a D8 Advance XRD diffractometer with Cu-Kα radiation (λ = 1.54184 Å, 40 kV and 40 mA) at a scanning rate of 10º/min. Infrared spectra were recorded on a Nicolet 5700 spectrometer, scanned from 4000 cm^{-1} to 400 cm^{-1}. Thermogravimetric (TG) measurement and Differential Thermal Analysis (DTA) was carried out using a Pyris Diamond TG/DTA instrument (Q600 SDT) under N_2 flow at 10°C min^{-1} in the temperature range 50–800°C. The textural properties of the samples were determined by nitrogen physisorption at liquid nitrogen temperature (–196°C) using a Quantachrome autosorb-iQ-2MP. The samples were degassed at 300°C for 5 h before the measurements. The pore textural properties including specific BET (Brunauer-Emmett-Teller) surface area were obtained by analyzing N_2 adsorption-desorption isotherm.

2.3. Adsorption experiments

A 10 mg/L perchlorate stock solution was prepared from $NaClO_4$. Perchlorate bearing solutions were synthesized by diluting the stock solution. Adsorbent dosage effect experiment was carried out in batch manner by putting various dosage of CHMAC (0.1–2.67 g/L) into 200 mL beaker flasks containing 150 mL of the perchlorate solution (2000 µg/L), respectively. These mixtures were shaken at a constant shaking speed of 200 rpm in a thermostat shaker at room temperature for 24 h. Solution pH was not controlled during the reaction.

The effect of different pH values on perchlorate adsorption was investigated by adding CHMAC (0.2 g) into 150 mL perchlorate solution (2000 µg/L) with varying initial pH values from 2 to 12. The pH values of perchlorate solution were adjusted with 1 M NaOH or 1 M HCl.

Adsorption isotherms were conducted with initial perchlorate concentrations of 500, 1000, 2000, 5000, 10000 and 20000 µg/L at 25°C and the contact time of 24 h. Solution pH was not controlled during the reaction.

The effect of contact time was carried out at specific time intervals of 5, 10, 15, 30, 60, 90, 120, 180, 200, 240, 540, 720, 1440, 2880 and 5760 min with the initial perchlorate concentration of 2000 µg/L at 25°C.

After adsorption, the mixed solution was taken 2 mL by syringe and filtered by 0.45µm membrane (nylon 66). The residual perchlorate in the filtrate was quantified using an ion chromatograph (Dionex, ICs2000) equipped with a suppressed conductivity detector, an AS20 column, an AG20 guard column, and a 250 µL sample loop (detection limit = 4 µg/L). A degassed 35 mmol/L sodium hydroxide solution was used as eluent.

All adsorption experiments were carried out in triplicate and the average data were used to evaluate adsorption activity.

The adsorption capacity of perchlorate q_e (mg/g) was calculated by the following equation:

$$q_e = (C_0 - C_t)\ V/M \tag{1}$$

where C_0 and C_t mean that initial concentration and concentration at any time (mg/L), respectively. M represents the amount of adsorbent (g). V is the volume of perchlorate solution (L).

3. Results and discussion

3.1. Characterization of MgAlCe hydrotalcite-like compounds

3.1.1. XRD analysis

The XRD patterns of the HMAC and CHMAC are shown in Fig. 1. It is found that all the diffraction patterns of HMAC5 and HMAC10 have the sharp and symmetric peaks at lower 2q (003, 006 and 012), indicating the formation of the typical hydrotalcite-like compounds [35]. Compared with MgAl-LDH, HMAC has two new peaks at 15.46º–16.17º, and a acromion peak at 22.92°. Moreover, the new peak intensities mainly corresponding to the amount of Ce in the product, which is due to the incorporation of Ce in the lattice framework. It is well known that the radius of Ce^{3+} (0.1 nm) is larger than that of Mg^{2+} (0.072 nm) and Al^{3+} (0.067 nm). When the Ce^{3+} partial substitution of Al^{3+} into the lattice, the new formed octahedron are larger than the surrounding MgAl octahedron, resulting in a protrusion of the original layer plane, which equivalent to the formation of a new plane layer. Therefore, higher the content of Ce results in higher protrusion of the original layer plane, which further leads to the formation of stronger diffraction peak intensity [36]. However, increasing Ce content to HMAC20, the diffraction peaks of hydrotalcite-like compounds disappears, which indicates that the addition of a large number of Ce is not favorable to the formation of hydrotalcite-like compounds. In addition, there is a weak peak at 2q value of about 28.5°, which corresponds to the characteristic peak of $Ce(OH)_3$ (JCPDS card no. 74–0665) [37].

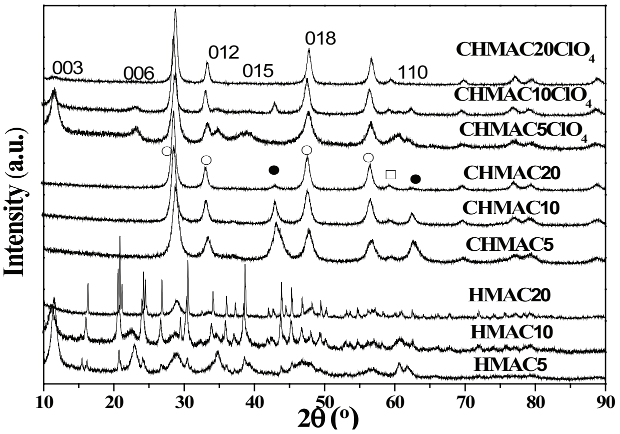

Fig. 1. XRD patterns of HMAC5, HMAC10, HMAC20, CHMAC5, CHMAC10, CHMAC20, and CHMAC after uptake of perchlorate (□, $MgAl_2O_4$ ○, CeO_2 ●, MgO).

When the HMAC is calcined at 600°C, the patterns of CHMAC only show the metal oxide diffraction peaks, which indicated that the hydrotalcite-like structure is severely destroyed. Upon adsorption of perchlorate, CHMAC5 and CHMAC10 again show unique characteristics as a result of reconstruction, which indicates that MgAlCe hydrotalcite-like compounds containing a small number of Ce has the "reformation effect" structure.

3.1.2. FT-IR analysis

FT-IR characterization of the HMAC, CHMAC and CHMAC after perchlorate adsorption is shown in Fig. 1S. In the FT-IR spectra of HMAC, the bands observed at 3500 cm^{-1} are due to the vibration of structural OH groups hydrogen bonded with interlamellar water molecules or OH groups in adjacent layers [38]. The weak peak at 1637 cm^{-1} is due to the water from the interlayer water. The band at 1384 cm^{-1} corresponded to the carbonate group. Compared with HMAC, the most obvious changes observed in the FT-IR spectra of CHMAC is the disappearance of bands at 1384 cm^{-1} and reappears during the adsorption of perchlorate, which indicates the surface adsorption of carbonate anions is a property of CHMAC [39]. The FT-IR results are in good agreement with above XRD results.

3.1.3. TG,DTA and BET analysis

The thermal behaviors of the HMAC and CHMAC after perchlorate adsorption are analyzed by TG and DTA experiments (Fig. 2). With the increase of temperature, TG can judge the material thermal decomposition, at the same time of material thermal decomposition, DTA will appear endothermic peak. It is found that both HMAC and CHMAC after perchlorate adsorption display mass loss at three temperature ranges. The first mass loss occurs from 50 to 200°C and is attributed to the removal of surface adsorbed and interlayer water molecules. The second mass loss occurs from 200 to 400°C, which is ascribed to the decomposition of the hydroxyl group and the layer CO_3^{2-}. The third mass loss occurs from 400 and 600ºC, which is due to the decomposition of interlayer anion. Interestingly, with the increase of Ce content, the mass loss rate of CHMAC after perchlorate adsorption gradually decreased. This indicates the decrease of the layer spacing and the anion content in the intercalated layer due to the incorporation of Ce, consequently resulting in the decrease of perchlorate adsorption content. In addition, the specific surface area of HMAC5 is 12.1 $m^2 \cdot g^{-1}$ and increases to 1003 $m^2 \cdot g^{-1}$ after calcination, which may be attributed to the formation of a large amount of irregular channels.

3.2. Perchlorate removal by MgAlCe hydrotalcite-like compounds

3.2.1. Effect of adsorbent dosage

The experimental results of removal efficiency (%) and adsorption capacity (μg/g) versus adsorbent dose (g/L)

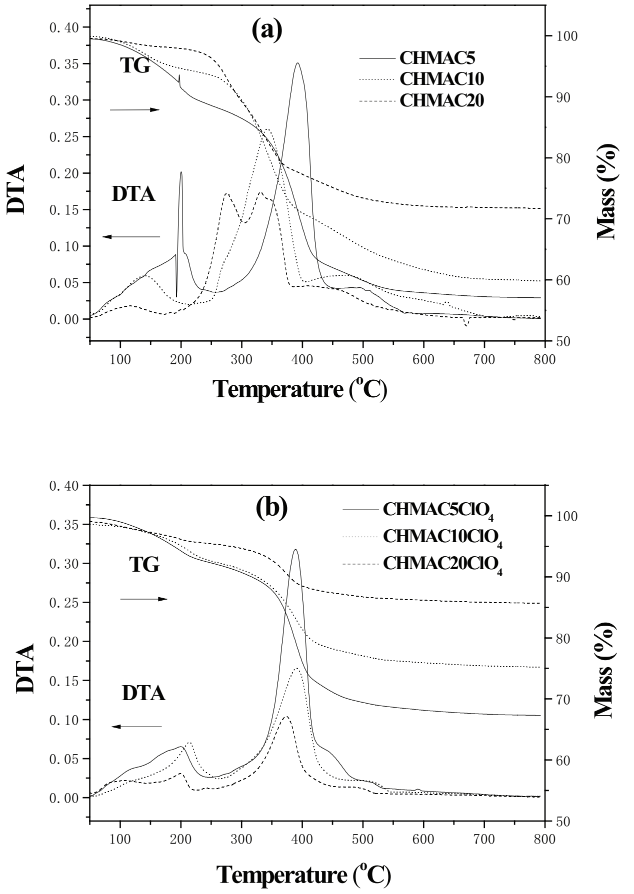

Fig. 2. TG and DTA profiles of HMAC5, HMAC10, HMAC20 (a) and CHMAC5ClO$_4$, CHMAC10ClO$_4$, CHMAC20ClO$_4$ (b).

are presented in Fig. 3. It is found that the adsorbent dose markedly influenced removal efficiency of perchlorate and adsorption capacity. A high CHMAC dose achieves a high perchlorate removal, which is consistent with previous results [27]. The higher dosage of CHMAC can provide a more number of available active sites to ClO$_4^-$, which leads to a greater removal rate. Moreover, with the increase of Ce loading in CHMAC, the removal rate and adsorption capacity both decrease, which further indicate the addition of excessive Ce is not conducive to remove perchlorate. In addition, with the increase of adsorbent dose, all CHMAC samples display a two-phase adsorption pattern. As CHMAC5 sample increases from 0.1 to 1.33 g/L, the removal rate of perchlorate is increased from 39% to 83%. Meanwhile, the adsorption capacity is linearly decreased from 7141 to 1143 µg/g. However, further increasing dosage of CHMAC5 to 2.67 g/L, both adsorption capacity and removal efficiency are tend to be equilibrium. Therefore, an adsorbent dose of 1.33 g/L is used as optimum dosage in the following tests.

3.2.2. *Effect of initial solution pH*

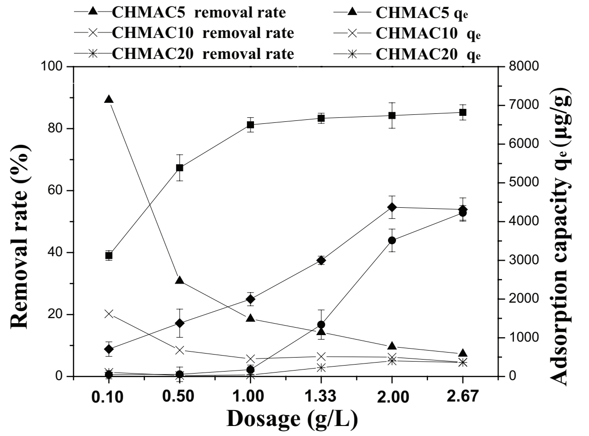

Fig. 3. Effect of dosage on perchlorate removal by CHMAC (initial concentration = 2000 µg/L, T = 25°C, pH = 6 , contact time = 24 h).

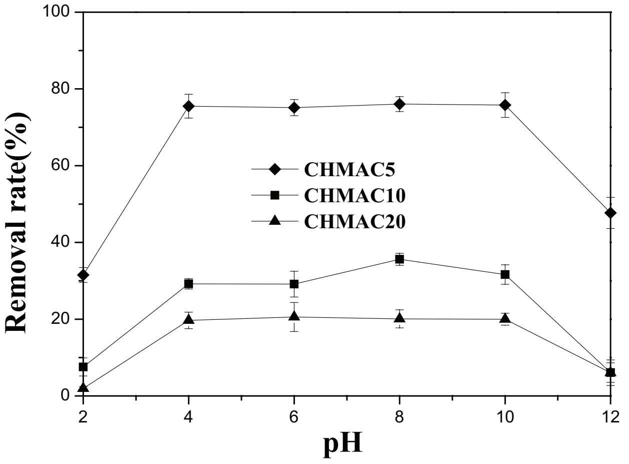

Fig. 4. Effect of initial pH value on the adsorption capacity (initial concentration = 2000 µg/L, T = 25°C, CHMAC adsorbent dosage = 1.33 g/L, contact time =24 h).

In order to evaluate the effect of the pH on the removal efficiency of the CHMAC, the adsorption batch at various pH (from 2 to 12) are conducted at 2000 µg/L initial concentration of perchlorate solution with 1.33 g/L CHMAC. As shown in Fig. 4, the highly effective perchlorate removal is observed in the broad pH range with the maximum removal occurring in the pH range 4–10. The initial solution pH has stronger effect on the perchlorate removal by CHMAC, and the removal rate decreases steeply in strong acidic solution (pH<4) or strong alkaline solution (pH>10). The removal rate of phosphate is lower at pH 4.0, probably due to dissolution of the adsorbents in acid medium [27]. As shown in Fig. 5, a high Mg^{2+} concentration is liberated into solution at strong acidic solution (pH<4), consequently resulting in the dissolution of the structure of CHMAC. Remarkably, at pH 4–10, CHMAC displays strong buffer ability, and the final solution pH is within a narrow range of 11.38–11.8 (Fig. 2S). Further increasing pH to strong alkaline (pH>10), the removal efficiency significantly decreased, which could be explained by the competition between the hydroxide and perchlorate onto the active site of CHMAC. The previous many results also prove above conclusion. In

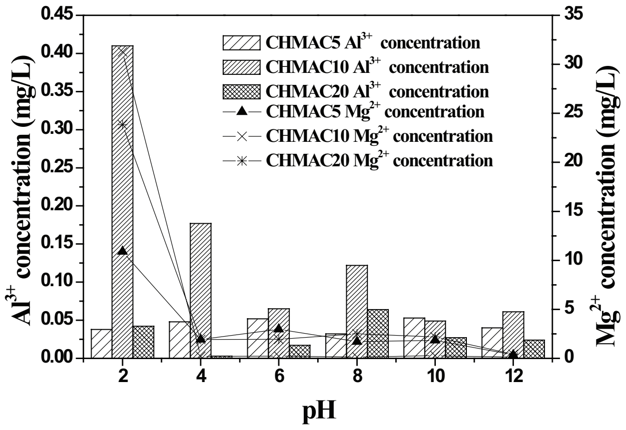

Fig. 5. Concentration of metal ions in resulting solution (initial concentration = 2000 μg/L, T = 25°C, CHMAC adsorbent dosage = 1.33 g/L, contact time = 24 h).

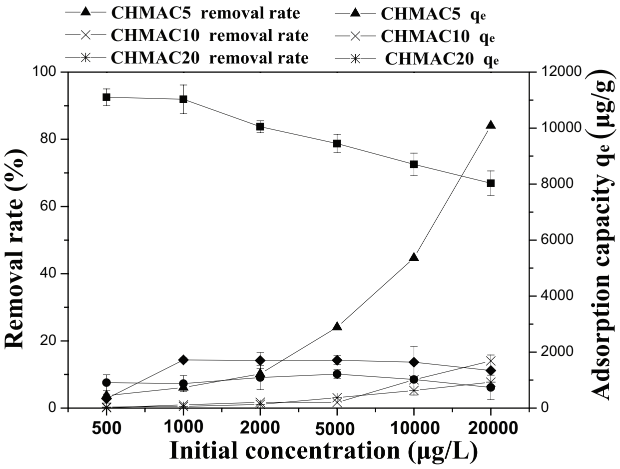

Fig. 6. Effect of initial concentrations on perchlorate removal (pH = 6, T = 25°C, CHMAC adsorbent dosage = 1.33 g/L, contact time = 24 h).

practical application, the pH of the wastewater or natural water is 4–9. At this range, the removal rate of phosphate adsorbed on CHMAC5 is more than 70%. Therefore, it does not need to adjust the solution pH in consideration of practical application, and initial pH 6 is selected as the optimum pH for further adsorption tests.

3.2.3. Effect of initial perchlorate concentration

Effect of initial perchlorate concentration (500–20,000 μg/L) on the adsorption capacity by CHMAC is presented Fig. 6. With the increase of initial perchlorate concentration, the adsorption capacity of CHMAC5 linearly increases. When initial concentration reaches 20,000 μg/L, CHMAC5 still have not reached saturation, which indicates that the addition of moderate Ce is beneficial to the improvement of the adsorption capacity. Compared with other hydrotalcite-like compounds, such as MgAlFe [27], our MgAlCe hydrotalcite-like compounds display higher adsorption capacity of perchlorate. In addition, the q_e for CHMAC5, CHMAC10, CHMAC20 are 10088 μg/g, 1685 μg/g, 929 μg/g respectively. This further indicates excessive Ce is not conducive to improve the adsorption capacity.

3.2.4. Effect of co-existing anions on perchlorate removal

Fig. 7 shows the effect of coexisting anions (CO_3^{2-}, PO_4^{3-}, NO_3^-, SO_4^{2-}, Cl^-) on perchlorate removal by CHMAC5. The concentrations of coexisting anions varied from 5 to 200 mg/L. It is found that all the anions both show an inhibiting effect on perchlorate adsorption by CHMAC5 with an order of $CO_3^{2-} > PO_4^{3-} > Cl^- > SO_4^{2-} > NO_3^-$. Here, due to the "reformation effect", the effect of CO_3^{2-} is especially significant. In other words, CO_3^{2-} ions have the priority to be adsorbed onto CHMAC5 to recover its initial structure. Previous studies showed the hydrotalcite had higher affinities for anions with greater charge density [40], i.e., multivalent anions are adsorbed more readily than monovalent anions. However, Cl^- is a special example. On the premise of the same quality, Small atomic weight of Cl^- results in the large molecular weight. In addition, with the increase of the concentration of coexisting anions, the inhibiting degree is gradually increased.

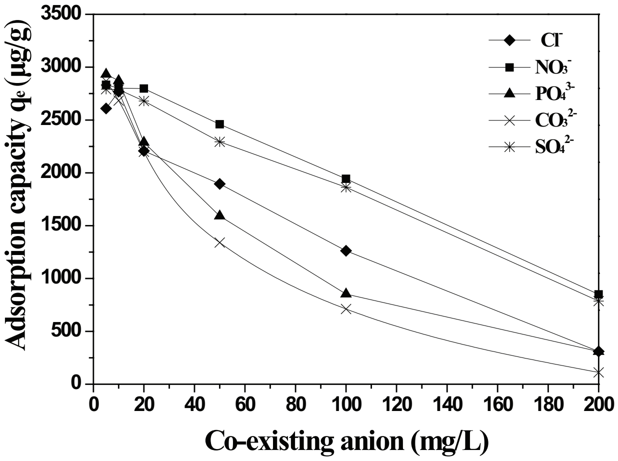

Fig.7. Effect of co-existing anions on perchlorate removal (initial concentration = 2000 μg/L, T = 25°C, CHMAC adsorbent dosage = 1.33 g/L, contact time = 24 h, pH = 6).

3.2.5. Effect of temperature and contact time

The effect of surroundings temperature on perchlorate adsorption by CHMAC5 is presented in Fig. 8a. It is found that adsorption capacity fast increases with the increase of surroundings temperature. Therefore, a significant effect of surroundings temperature on perchlorate adsorption is discovered, indicating that the adsorption process is kinetically controlled by an endothermic process. Similar results were reported by other researchers [26,41]. In addition, the effect of contact time on perchlorate adsorption using CHMAC5 is shown in Fig. 8b. The adsorption capacity increases rapidly in the first 12 h and gradually reaches equilibrium at about 24 h. With the increase of contract time, the rate of

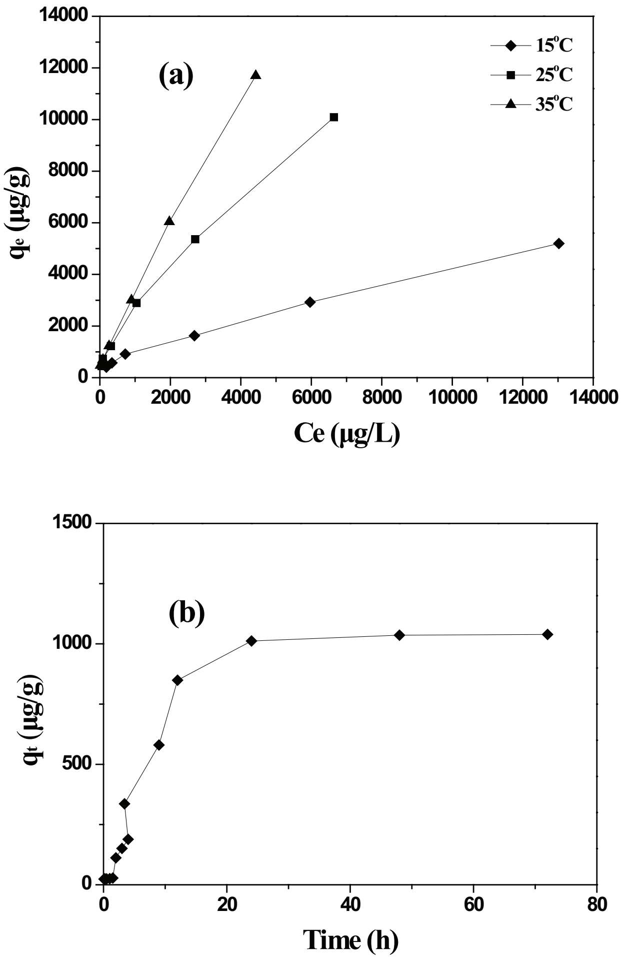

Fig. 8. Effect of temperature (a) and contact time (b) on perchlorate removal (initial concentration = 2000 µg/L, CHMAC adsorbent dosage = 1.33 g/L, pH = 6).

perchlorate adsorption decreases, which can attribute to the decrease in the number of activated adsorption sites.

3.3. Equilibrium isotherms for perchlorate adsorption

The isotherm models of Linear [Eq.(2)] [42], Langmuir [Eq. (3)] [43], Freundlich [Eq. (4)] [43] and Temkin [Eq. (5)] [44] are investigated to determine the experimental adsorption equilibrium data of perchlorate on CHMAC adsorbents.

$$q_e = K_r C_e + b \tag{2}$$

$$q_e = K_r C_e + b \tag{3}$$

$$q_e = K_F C_e^n \tag{4}$$

$$q_e = B \ln A + B \ln C_e \tag{5}$$

where q_e is the amount of perchlorate adsorbed (µg/g), K_r is the binding energy of the adsorption system (L/µg), b is the linear constant, C_e is the equilibrium concentration perchlorate (µg/L), q_{max} is the maximum adsorption capacity (µg/g), d is the Langmuir constant, K_F is the Freundlich constant, n is the adsorption intensity, B and A are the Temkin constants.

The adsorption isotherms and fitting results are shown in Fig. 3S and Table 1. As seen, the Freundlich isotherm was the best one to describe perchlorate adsorption on CHMAC at 25ºC with the highest R^2 of 0.9931 (CHMAC5), 0.9444 (CHMAC10) and 0.9793 (CHMAC20).

3.4. Adsorption kinetics

In order to study perchlorate adsorption mechanism of CHMAC5, the pseudo-first order model [45], the pseudo-second order model [46], the Elovich equation model [47], and inter-particle diffusion model [48] with equations from (6) to (9) are examined to fit the experimental data, respectively.

$$\ln(q_e - q_t) = \ln q_e - k_1 t \tag{6}$$

$$\frac{t}{q_t} = \frac{1}{k_2 q_e^2} + \frac{t}{q_e} \tag{7}$$

$$q_t = \beta \ln(\alpha\beta) + \beta \ln t \tag{8}$$

$$q_t = k_i t^{0.5} \tag{9}$$

where q_e and q_t are the adsorption capacity of perchlorate on the adsorbent (µg/g) at equilibrium and at time t (min), respectively; k_1 (min^{-1}) is the rate constant of pseudo-first-order adsorption; t is the reaction time; k_2 (g/µg min) is the rate constant of pseudo-second-order adsorption; α and β are the initial adsorption rate (µg/g min) and the desorption constant (g/µg), respectively; k_i (µg/g min$^{0.5}$) is the intraparticle diffusion rate.

Measured data and modeled data in the kinetics tests for perchlorate adsorption are presented in Fig. 4S and Table 2. The order of four kinetics models with regards toward the fitting of measured and modeled data is the first-order kinetics model > the inter-particle diffusion model > the Elovich equation model > the pseudo-second-order kinetics model according to coefficient of determination (R^2). Above results show that the pseudo-first-order kinetics model appears to be better describing the kinetic process of perchlorate adsorption onto CHMAC5.

3.5. Thermodynamic parameters

The perchlorate adsorption of CHMAC5 is measured at three different temperatures (15, 25 and 35°C) under the optimized condition and thermodynamic parameters such as Gibbs free energy (ΔG°), standard entropy change (ΔS°) and standard enthalpy change (ΔH°) are calculated from Eqns. (10)–(11) and showed in Table 3 [49].

$$\Delta G^\circ = -RT \ln (K_L) \tag{10}$$

$$\Delta G^\circ = \Delta H^\circ - T\,\Delta S^\circ \tag{11}$$

Table 1
Calculated equilibrium constants for adsorption of perchlorate on CHMAC with different temperature

T (°C)	CHMAC (%)	Linear			Langmuir			Freundlich			Temkin		
		K_r (L/μg)	*b*	R^2	K_L (L/mg)	q_m (μg/g)	R^2	K_F ((μg/g) (L/μg)$^{1/n}$)	*n*	R^2	*A*	*B*	R^2
15	5	0.2952	798.06	0.9873	7.95782×10^{-5}	12500	0.8148	15.027	0.6184	0.9932	0.002841	1767.3	0.8125
	10	0.0415	34.023	0.9026	-1.24493×10^{-5}	–2000	0.1875	0.0045	1.2323	0.9724	0.000735	427.9	0.8054
	20	0.083	190.49	0.9318	-4.67545×10^{-6}	–16667	0.0378	0.0304	1.1253	0.9683	0.000833	864.38	0.8932
25	5	1.4376	860	0.9846	0.000414508	12500	0.8463	41.248	0.6166	0.9931	0.013517	1741.5	0.8239
	10	0.0978	–18.235	0.9543	-3.66418×10^{-5}	–1250	0.1217	0.0157	1.194	0.9444	0.001115	451.48	0.7966
	20	0.0495	65.939	0.9476	1.42714×10^{-5}	5000	0.3407	0.0794	0.9761	0.9793	0.0013	262.29	0.9476
35	5	2.555	597.06	0.9973	0.00040107	16666.7	0.6408	69.033	0.5774	0.9447	0.025127	1728.5	0.7035
	10	0.4879	55.347	0.9911	-1.24844×10^{-5}	–33333	0.1458	0.217	1.0994	0.9797	0.001632	1624	0.8848
	20	0.4989	120.44	0.9823	-9.43619×10^{-6}	–50000	0.0322	0.3358	1.0543	0.9661	0.001754	1630.3	0.8854

Table 2
Kinetics models parameters for adsorption of perchlorate on CHMAC5

Initial concentration	Quasi first order kinetic model			Quasi second order kinetic model			Elovich equation			Particles diffusion model	
(mg/L)	k_1 (min^{-1})	q_e (μg/g)	R^2	k_2	$q_{e\cdot cal}$ (μg/g)	R^2	α (μg/gmin)	β (μg/gmin)	R^2	k_i (μg/gmin)	R^2
2	0.0021	1141.3	0.9773	3.41×10^{-7} (g/μgmin)	1666.7	0.508	2.49×10^{-5}	181.7	0.8	19.252	0.8595

Table 3
Thermodynamic parameters for adsorption of perchlorate on CHMAC5

T (°C)	ΔG° (kJ/mol)	ΔH° (kJ/mol)	ΔS°(J/mol/K)
15	–6.49	56.41	218.98
25	–9.22		
35	–10.84		

where T is temperature (K), *R* is universal gas constant, and K_L (L/mg) is Langmuir constant.

The negative value of ΔG° at all temperatures shows the spontaneity of ongoing adsorption. With the increase of temperature, a decrease in value of ΔG° is found, which indicates the higher temperature favors perchlorate adsorption. The positive value of ΔS° suggests that disorder at the solid-solution interface increases during perchlorate adsorption. The positive value of ΔH° further indicates the endothermic nature of the process.

3.6. Adsorption mechanism

The adsorption mechanism of perchlorate by CHMAC is investigated by the structural characterization of HMAC, CHMAC and the reconstructed HMAC with perchlorate. XRD results indicate that the diffraction peaks of the hydroxide layer structure of (003), (006), and (012) disappear after the HMAC with low Ce content are calcined to CHMAC at 600°C, suggesting that the layered structure of parent HMAC was destroyed when heated at 600°C [50]. However, the layer structures of the parent HMAC are reconstructed subsequent to the adsorption of perchlorate by the CHMAC. In addition, FTIR spectra shows that the peak at 1384 cm^{-1}, corresponded to the carbonate group, disappears after calcination and reappears during the adsorption of perchlorate. Above results indicates that the "reformation effect" (i.e. the reconstruction of HMAC with perchlorate as an interlayer anion) plays an important role in the adsorption of perchlorate by the CHMAC. When heated at 600°C, the layered structure of parent HMAC was destroyed due to interlayer root anionic carbonate decomposition and decomposition of the original LDH into mixed oxide of magnesium, aluminum and cerium during the calcinations. In the process of adsorption of perchlorate, perchlorate enters into the layers and layer structure restores.

4. Conclusions

In summary, the calcination product of MgAlCe hydrotalcite-like compounds was a promising adsorbent for anionic perchlorate pollutant. The characterization results indicated that carbonate layered double hydroxides of HMAC were lost during calcination at 550ºC, but were reconstructed subsequent to adsorption of perchlorate, which was primary driven by the "reformation effect" of HMAC with perchlorate as an interlayer anion. The calcination temperature of 600ºC and a molar ratio of Mg/Al/Ce at 3:0.8:0.2 (CHMAC 5%) were the optimal conditions for the adsorbent preparation. In addition, the solution chemistry factors including adsorbent dosage, initial solution pH, initial perchlorate concentration, co-existing anions, temperature and contact time could affect the efficiencies of perchlorate adsorption to the different CHMAC. Both CHMAC5 % and CHMAF10% could reduce 85% perchlorate within 300 min at a broad initial pH range of 4.0–10.0 when initial perchlorate concentration is 2000 µg/L. The presence of Ce^{3+} in hydrotalcite would increase the attraction of perchlorate in the interlayer by layers and suppress the concentration of dissolved metal. Freundlich models better explained the perchlorate adsorption data at 25°C. Such an adsorption kinetics pattern could be well described by a pseudo-second-order reaction model. The adsorption process was endothermic and spontaneous in nature. The CHMAC as a novel nanoadsorbent exhibits a bright future for practical applications in perchlorate removal from the wastewater.

Acknowledgements

This work was sponsored financially by the National Natural Science Foundation of China (No. 51508327, 21507086) and Shanghai Sailing Program (14YF1409900, 16YF1408100).

References

[1] M. Sharbatmaleki, J.R. Batista, Multi-cycle bioregeneration of spent perchlorate containing macroporous selective anion-exchange resin, Water Res., 46 (2011) 21–32.

[2] Z.Q. Yang, O. Xiao, B. Chen, L.X. Zhang, H.G. Zhang, X.J. Niu, S.Q. Zhou, Perchlorate adsorption from aqueous solution on inorganic-pillared bentonites, Chem. Eng. J., 223 (2013) 31–39.

[3] E.T. Urbansky, Perchlorate chemistry: implications for analysis and remediation, Biochem. J., 2 (1998) 81–95.

[4] R.T. Wilkin, D.D. Fine, N.G. Burnett, Perchlorate behavior in municipal lake following fireworks displays, Environ. Sci. Technol., 41 (2007) 3966–3971.

[5] H. Ma, N.A. Bonnie, M. Yu, S. Che, Q. Wang, Biological treatment of ammonium perchlorate-contaminated wastewater: A review, J. Water Reuse Desal., 6 (2015) 82–107.

[6] D.R. Parker, A.L. Seyfferth, B.K. Reese, Perchlorate in groundwater: a synoptic survey of ‘‘pristine’’ sites in the coterminous United States, Environ. Sci. Technol., 42 (2008) 1465–1471.

[7] J.S. Traugott, F. Jessika, J.P. Carol, Untersuchung ausgewählter Oberflächen-, Grundund Bodenwasserproben auf Perchlorat in Deutschland: Erste Ergebnisse, Grundwasser-Zeitschrift der Fachsektion, Hydrogeologie, 16 (2011) 37–43.

[8] K. Kannan, M.L. Praamsma, J.F. Oldi, T. Kunisue, R.K. Sinha, Occurrence of perchlorate in drinking water, groundwater, surface water and human saliva from India, Chemosphere, 76 (2009) 22–26.

[9] O. Quiñones, J.E. Oh, B. Vanderford, J.H. Kim, J. Cho, S.A. Snyder, Perchlorate assessment of the Nakdong and Yeongsan watersheds, Republic of Korea, Environ. Toxicol. Chem., 26 (2007) 1349–1354.

[10] K. Kosaka, M. Asami, Y. Matsuoka, M. Kamoshita, S. Kunikane, Occurrence of perchlorate in drinking water sources of metropolitan area in Japan, Water Res., 41 (2007) 3474–3482.

[11] Q. Wu, T. Zhang, H.W. Sun, Perchlorate in tap water, groundwater, surface waters, and bottled water from China and its association with other inorganic anions and with disinfection byproducts, Arch. Environ. Contam. Toxicol., 58 (2010) 543–550.

[12] A.M. Leung, E.N. Pearce, L.E. Braverman, Environmental perchlorate exposure: potential adverse thyroid effects, Curr. Opin. Endocrinol. Diabetes Obesity, 21 (2014) 372–376.

[13] L. Ye, H. You, J. Yao, H. Su, Water treatment technologies for perchlorate: A review, Desalination, 298 (2012) 1–12.

[14] K. Karageorgiou, M. Paschalis, G.N. Anastassakis, Removal of phosphate species from solution by adsorption onto calcite used as natural adsorbent, J. Hazard. Mater., 139 (2007) 447–452.

[15] J.H. Xu, N.Y. Gao, D.Y. Zhao, D.Q. Yin, H. Zhang, Y.Q. Gao, W. Shi, Comparative study of nano-iron hydroxide impregnated granular activated carbon (Fe–GAC) for bromate or perchlorate removal, Sep. Purif. Technol., 147 (2015) 9–16.

[16] K. Kuzawa, Y.J. Jung, Y. Kiso, T. Yamada, M. Nagai, T.G. Lee, Phosphate removal and recovery with a synthetic hydrotalcite as an adsorbent, Chemosphere, 62 (2006) 45–52.

[17] T. Li, Z.Q. Yang, X.P. Zhang, N.W. Zhu, X.J. Niu, Perchlorate removal from aqueous solution with a novel cationic metal–organic frameworks based on amino sulfonic acid ligand linking with Cu-4,40-bipyridyl chains, Chem. Eng. J., 281 (2015) 1008–1016.

[18] L. Zeng, X.M. Li, J.D. Liu, Adsorptive removal of phosphate from aqueous solutions using iron oxide tailings, Water Res., 38 (2004) 1318–1326.

[19] R. Chitrakar, S. Tezuka, A. Sonoda, K. Sakane, K. Ooi, T. Hirotsu, Selective adsorption of phosphate from seawater and wastewater by amorphous zirconium hydroxide, J. Colloid Interface Sci., 297 (2006) 426–433.

[20] Z. Xiong, D.Y. Zhao, G. Pan, Rapid and complete destruction of perchlorate in water and ion-exchange brine using stabilized zero-valent iron nanoparticles, Water Res., 41 (2007) 3497–3505.

[21] A.M. Moore, C.H. De Leon, T.M. Young, Rate and extent of aqueous perchlorate removal by iron surfaces, Environ. Sci. Technol., 37 (2003) 3189–3198.

[22] B.P. Vellanki, B. Batchelor, Perchlorate reduction by the sulfite/ultraviolet light advanced reduction process, J. Hazard. Mater., 262 (2013) 348–356.

[23] X. Yu, C. Amrhein, R.M. Markatsumoto, Perchlorate reduction by autotrophic bacteria in the presence of zero-valent iron, Environ. Sci. Technol., 40 (2006) 1328–1334.

[24] K.H. Goh, T.T. Lim, Z.L. Dong, Application of layered double hydroxides for removal of oxyanions: a review, Water Res., 42 (2008) 1343–1368.

[25] Y. Zhang, S. Jing, H.Y. Liu, Reactivity and mechanism of bromate reduction from aqueous solution using Zn–Fe(II)–Al layered double hydroxides, Chem. Eng. J., 266 (2015) 21–27.

[26] T.F. Lv, W. Ma, G. Xin, R. Wang, J. Xu, D.M. Liu, F.J. Liu, D.C. Pan, Physicochemical characterization and sorption behavior of Mg-Ca-Al (NO_3) hydrotalcite-like compounds toward removal of fluoride from protein solutions, J. Hazard. Mater., 237–238 (2012) 121–132.

[27] Y.Q. Yang, N.Y. Gao, W.H. Chu, Y.J. Zhang, Y. Ma, Adsorption of perchlorate from aqueous solution by the calcination product of Mg/(Al-Fe) hydrotalcite-like compounds, J. Hazard. Mater., 210 (2012) 318–325.

[28] K. Yang, L.G. Yan, Y.M. Yang, S.J. Yu, R.R. Shan, H.Q. Yu, B.C. Zhu, B. Du, Adsorptive removal of phosphate by Mg–Al and Zn–Al layered double hydroxides: Kinetics, isotherms and mechanisms, Sep. Purif. Technol., 124 (2014) 36–42.

[29] Y.J. Lin, Q.L. Fang, B.L. Chen, Perchlorate uptake and molecular mechanisms by magnesium/aluminum carbonate layered double hydroxides and the calcined layered double hydroxides, Chem. Eng. J., 237 (2014) 38–46.

[30] M.P. Bernardo, F.K.V. Moreira, L.A. Colnago, C. Ribeiro, Physico-chemical assessment of [Mg-Al-PO_4]-LDHs obtained by structural reconstruction in high concentration of phosphate, Colloids Surf. A, 497 (2016) 53–62.

[31] Y.J. Lin, Q.L. Fang, B.L. Chen, Metal composition of layered double hydroxides (LDHs) regulating ClO_4^- adsorption to calcined LDHs via the memory effect and hydrogen bonding, J. Environ. Sci., 26 (2014) 493–501.

[32] L.G. Yan, K. Yang, R.R. Shan, T. Yan, J. Wei, S.J. Yu, H.Q. Yu, B. Du, Kinetic, isotherm and thermodynamic investigations of phosphate adsorption onto core–shell Fe_3O_4@LDHs composites with easy magnetic separation assistance, J. Colloid Interf. Sci., 448 (2015) 508–516.

[33] A. Halajnia, S. Oustan, N. Najafi, A.R. Khataee, A. Lakzian, Adsorption-desorption characteristics of nitrate, phosphate and sulfate on Mg-Al layered double hydroxide, Appl. Clay Sci., 80–81 (2013) 305–312.

[34] Guidelines for Drinking Water Quality, Recommendations World Health Organisation (second ed., addendum to vol. 1), World Health Organisation, Geneva (1998) 3.

[35] F. Cavani, F. Trifiro, A. Vaccari, Hydrotalcite-type anionic clays: preparation, properties and applications, Catal. Today, 11 (1991) 173–301.

[36] L.S. Li, J.B. Hui, X.S. Liu, X.X. Liu, Synthesis and characterization of hydrotalcite- containing rare earth, Chem. J. Chin. Univ., 14 (1993) 1048–1050.

[37] S. Yi, Z.H. Yang, S.W. Wang, D.R. Liu, S.Q. Wang, Q.Y. Liu, W.W. Chi, Effects of MgAlCe-CO_3 layered double hydroxides on the thermal stability of PVC resin, J. Appl. Polym. Sci., 119 (2011) 2620–2626.

[38] M.A. Ulibarri, I. Pavlovic, C. Barriga, M.C. Hermosín, Adsorption of anionic species on hydrotalcite-like compounds: effect of interlayer anion and crystallinity, Appl. Clay Sci., 18 (2001) 17–27.

[39] J.I.D. Cosimo, V.K. Diez, M. Xu, E. Iglesia, C.R. Apesteguia, Structure and surface and catalytic properties of Mg-Al basic oxides, J. Catal., 178 (1998) 499–510.

[40] L. Lv, J. He, M. Wei, D.G. Evans, X. Duan, Factors influencing the removal of fluoride from aqueous solution by calcined Mg-Al-CO_3 layered double hydroxides, J. Hazard. Mater., 133 (2006) 119–128.

[41] M.G. Sujana, G. Soma, N. Vasumathi, S. Anand, Studies on fluoride adsorption capacities of amorphous Fe/Al mixed hydroxides from aqueous solutions, J. Fluorine Chem., 130 (2009) 749–754.

[42] A. Agrawal, K.K. Sahu, B.D. Pandey, A comparative adsorption study of copper on various industrial solid wastes, AIChE J., 50 (2004) 2430–2438.

[43] S. Pradhan, S.S. Shukla, K.L. Dorris, Removal of nickel from aqueous solutions using crab shells, J. Hazard. Mater. B., 125 (2005) 201–204.

[44] S. Deng, Y.P. Ting, Fungal biomass with grafted poly (acrylic acid) for enhancement of Cu(II) and Cd(II) biosorption, Langmuir, 21 (2005) 5940–5948.

[45] N.K. Lazaridis, D.D. Asouhidou, Kinetics of sorptive removal of chromium (VI) from aqueous solutions by calcined Mg–Al–CO_3 hydrotalcite, Water Res., 37 (2003) 2875–2882.

[46] Y.S. Ho, G. Mckay, Sorption of dye from aqueous solution by peat, Chem. Eng. J., 70 (1998) 115–124.

[47] G. McKay, Y.S. Ho, J.C.Y. Ng, Biosorption of copper from waste waters: a review, Sep. Purif. Meth., 28 (1999) 87–125.

[48] M. Jansson-Charrier, E. Guibal, J. Roussy, Vanadium sorption by chitosan: kinetics and equilibrium, Water Res., 30 (1996) 465–475.

[49] L. Lv, P.D. Sun, Z.Y. Gu, H.G. Du, X.J. Pang, X.H. Tao, R.F. Xu, L.L. Xu, Removal of chloride ion from aqueous solution by ZnAl-NO_3 layered double hydroxides as anion-exchanger, J. Hazard. Mater., 161 (2009) 1444–1449.

[50] X. Yuan, Y. Wang, J. Wang, C. Zhou, Q. Tang, X.B. Rao, Calcined graphene/MgAl-layered double hydroxides for enhanced Cr(VI) removal, Chem. Eng. J., 221 (2013) 204–213.

Supplementary

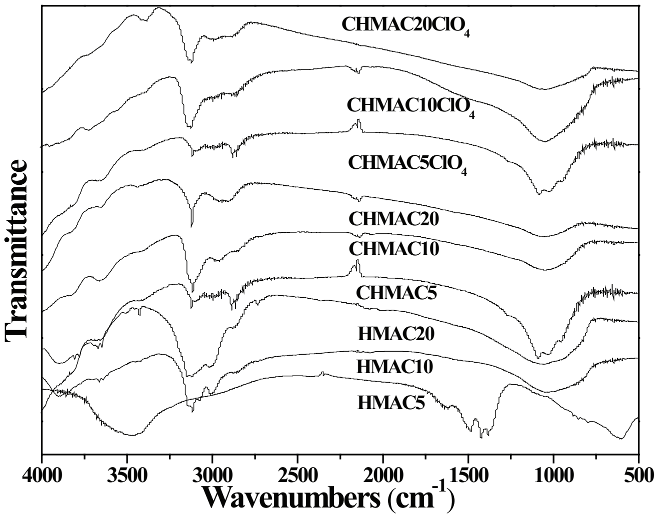

Fig. 1S. FT-IR spectra of HMAC5, HMAC10, HMAC20, CHMAC5, CHMAC10, CHMAC20, and CHMAC after uptake of perchlorate.

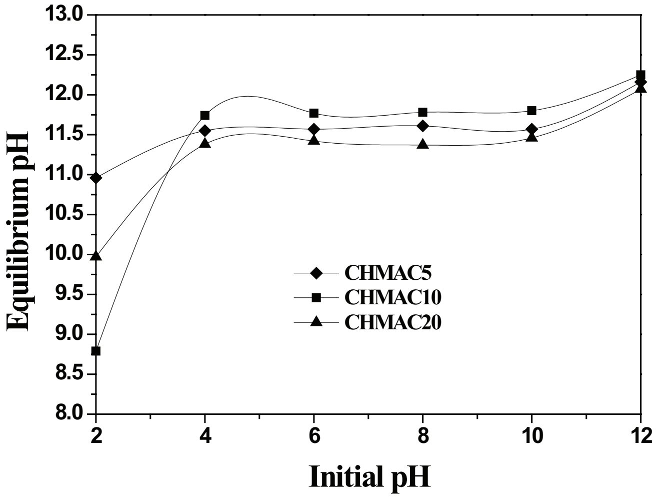

Fig. 2S. Effect of CHMAC on the equilibrium pH (initial concentration = 2000 µg/L, T = 25°C, CHMAC adsorbent dosage = 1.33 g/L, contact time = 24 h).

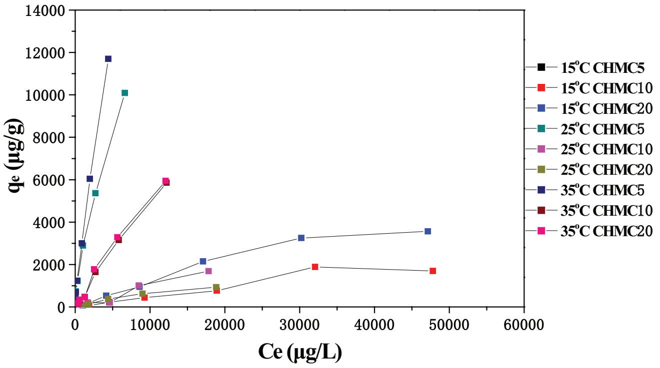

Fig. 3S. Isotherm adsorption of perchlorate by CHMAC at different temperatures.

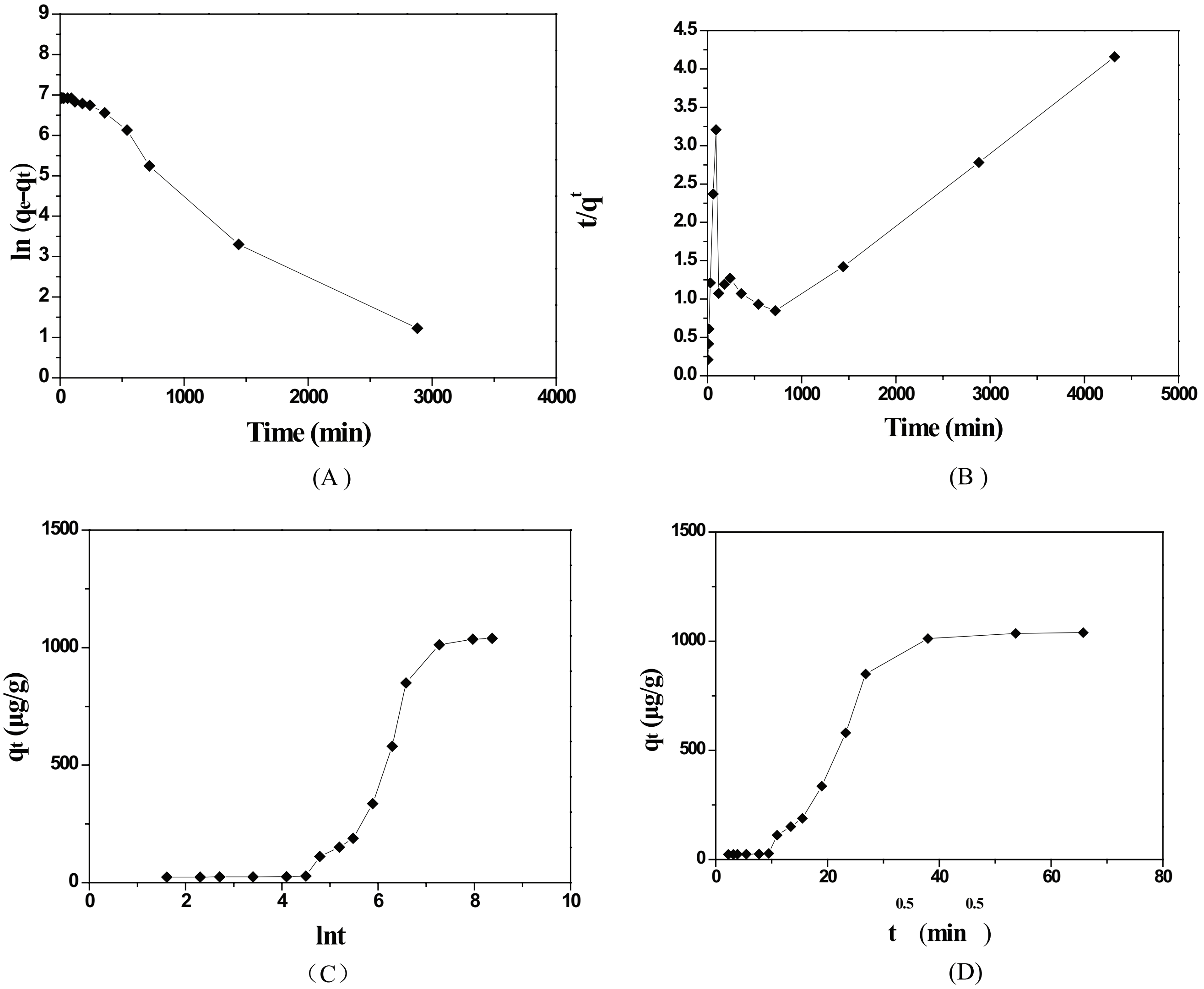

(A) (B) (C) (D)

Fig. 4S. (a) First-order kinetics model, (b) pseudo-second-order kinetics model, (c) Elovich equation model, (d) inter-particle diffusion model of CHMAC5 (initial concentration = 2000 μg/L, T = 25°C, CHMAC adsorbent dosage = 1.33 g/L, contact time = 24 h, pH = 6).